Quasiprobability distributions for the Jaynes-Cummings model with cavity damping

J. Eiselt and H. Risken
Abteilung für Theoretische Physik, Universität Ulm, W-7900 Ulm, Germany
(Received 16 August 1990)

The Jaynes-Cummings model with cavity damping is investigated in the rotated-wave approximation. First we introduce six appropriate combinations of the matrix elements of the density operator, which are still operators with respect to the light field. With the help of the s-parametrized quasiprobability distributions of Cahill and Glauber [Phys. Rev. **175**, 1882 (1969)] the equations of motion for the density operator transform to six coupled partial-differential equations. By expanding the quasiprobability distributions into two suitable sets, we obtain six tridiagonally coupled differential equations for the expansion coefficients, which are solved by a Runge-Kutta method. Starting with an initial coherent state of the cavity field and the atom in its upper state, we find that the initially one-peak quasiprobability function splits into two peaked functions counterrotating in the complex plane and, depending on the damping constant, spiraling into the origin. Revivals of the inversion oscillation are found for those times, when the two peaks collide. The time dependence of the inversion and the intensity as well as some special distributions of interest are also discussed.

I. INTRODUCTION

A fundamental problem in quantum optics is the interaction of light with matter. One of the simplest models describing this interaction is the Jaynes-Cummings (JC) model,[1] where a single two-level atom interacts with one light mode of the cavity. In the rotating-wave approximation this model can be solved exactly. Starting with a cavity field in a coherent state $|\alpha_0\rangle$ and with the atom in its upper state it was found that repeated decays and revivals of Rabi oscillations occur, see for instance Refs. 1–6, and that for certain times the field mode shows squeezing.[7–9] The predicted collapses and revivals of the inversion oscillations are in agreement with the experiments done with Rydberg atoms in a microwave cavity; see Refs. 10 and 11.

In the experiments, the damping of the cavity mode and the number of thermal microwave photons $n_{\rm th}$ are not negligibly small. Thus for a detailed comparison with experiments, cavity damping must be included in a treatment of the JC model. With cavity damping one has to solve an appropriate equation for the density operator, which describes the system. This equation of motion for the density operator is more difficult to solve. As far as we know, no analytic solution seems to exist. (An even simpler model, the so-called Raman coupled model,[12] however, can be solved analytically also with the inclusion of cavity damping.[13]) In the JC model damping was already included by some approximation technique valid for small damping and $n_{\rm th}=0$ (dressed atom approximation), see Refs. 14–16, or numerically without any such approximation.[17] In the last reference, an initial intensity of the coherent field of $I_0 = |\alpha_0|^2 = 2$ has been used. This number is too small to give pronounced repeated decays and revivals of the Rabi oscillations without detuning. For an appreciable detuning, however, the revivals can be seen even for this low initial intensity.[17] With the method presented below initial intensities up to $I_0=30$ can be handled.

The main goal of the present work is the calculation of the quasiprobability distributions of the light field. (In the references on the JC model mentioned so far no quasiprobability distributions have been calculated.) Here we use the s-parametrized quasiprobability distributions of Cahill and Glauber.[18] By specializing the parameter s, the usual P, Wigner, and Q functions are obtained. With the help of the quasiprobability distributions one gains new insight into the mechanism of the interaction of the single atom with the light mode. The main result is the following: Starting with a light field in a coherent state $|\alpha_0\rangle$ and with the atom in its upper state the initial shifted Gaussian quasiprobability distribution splits into peaks counterrotating in the complex α plane on a circle with a radius given by given $\sqrt{I_0}$. After the splitting one has a decay of the Rabi oscillations of the inversion. At the opposite side of the circle the peaks collide. At this time one observes the revival of the Rabi oscillations. Then the distribution splits again into two peaks till they collide again at the original site of the circle and so forth. The collision of the peaks is connected with the revivals of the Rabi oscillations. This effect is found even without damping. With damping the counterrotating peaks spiral into the origin till finally the stationary distribution is reached. Without damping the Q function can be given analytically in terms of an infinite sum, see Appendix A, and already shows this splitting.[19]

Without damping a splitting was also found in the Raman coupled model by Phoenix and Knight.[20] In this model a closed expression for the infinite sums can easily be obtained.[20] As shown recently by Schoendorff and one of us[13] the quasiprobability distribution and in particular the splitting can be given analytically even for arbitrary cavity damping constants for the Raman coupled model.

The main procedure for calculating the quasiprobabil-

ity distributions is as follows. First we introduce the four matrix elements of the density operator with respect to the two-level atomic states. These matrix elements are still operators with respect to the light field. Next we form six suitable combinations of these matrix elements. As it will turn out later on, these combinations lead to more simple recurrence relations than the four original ones. The equation of motion for the density operator then leads to a closed system of six coupled equations for the six combinations. With the help of the quasiprobability distributions of Cahill and Glauber,[18] the equations of motion are then transformed to coupled partial-differential equations for the quasiprobability distributions. A suitable expansion of these distributions into two complete sets finally leads to a system of ordinary differential equations for the expansion coefficients. Because of the introduction of the six combinations these equations are tridiagonally coupled in only one index. By using a Runge-Kutta integration procedure for the tridiagonally coupled equations we thus obtain the quasiprobability distributions. In addition, we also obtain the inversion and the mean intensity as well as other moments as a function of time. This procedure and some of the main results have been reported in Refs. 21 and 22.

The paper is organized as follows. In Sec. II the equation of motion for the density operator, its atomic matrix elements, and the six combinations and their equations of motion are given. These combinations are still operators with respect to the light field. In Sec. III we introduce the quasiprobability distributions and show that the coupled equations of motion for the combinations are transformed into coupled partial-differential equations. In Sec. IV the quasiprobability distributions are expanded into two suitable sets, which finally leads to a system of tridiagonally coupled ordinary differential equations for the expansion coefficients. In Sec. V we solve these tridiagonally coupled equations with the Runge-Kutta procedure and present the results for inversion, mean intensity, variance, and various quasiprobability distributions. In Sec. VI the photon distribution, the distribution of the rotated quadrature phase as well as of the phase are presented. Finally in Sec. VII we summarize our results.

II. DAMPED JC MODEL AND ITS EQUATION OF MOTION

As already mentioned the Jaynes-Cummings model consists of a single two-level atom, coupled to a single cavity mode. The Hamiltonian of this system reads, in the rotating-wave approximation,[1] see also Ref. 23,

$$H/\hbar = \omega_c a^\dagger a + \omega_a \sigma_z/2 + g(a\sigma^+ + a^\dagger \sigma^-) , \qquad (2.1)$$

where σ_z, σ^+, and σ^- are the Pauli spin matrices, $a^\dagger$ and a are the creation and annihilation operators of the light mode, ω_a and ω_c are the frequencies of the atom and of the cavity mode respectively, and g is the coupling constant. In the presence of cavity damping with a decay rate κ the equation of motion for the density operator $\rho = \rho(t)$ of the system takes the form

$$\dot{\rho} = -i[H/\hbar, \rho] + \kappa L_{\rm ir}(\rho) , \qquad (2.2)$$

where $L_{\rm ir}$, which describes the irreversible motion caused by cavity damping, is given by

$$\begin{aligned} L_{\rm ir}(\rho) &= 2a\rho a^\dagger - \rho a^\dagger a - a^\dagger a \rho + 2n_{\rm th}[[a,\rho],a^\dagger] \\ &= (n_{\rm th}+1)(2a\rho a^\dagger - \rho a^\dagger a - a^\dagger a\rho) \\ &\quad + n_{\rm th}(2a^\dagger \rho a - \rho a a^\dagger - a a^\dagger \rho) . \end{aligned} \qquad (2.3)$$

In (2.3) $n_{\rm th} = 1/\{\exp[\hbar\omega_c/(kT)] - 1\}$ is the number of thermal quanta. In the interaction picture

$$\exp[i\omega_c(a^\dagger a + \sigma_z/2)t]\ \rho\ \exp[-i\omega_c(a^\dagger a + \sigma_z/2)t] \Rightarrow \rho \qquad (2.4)$$

we obtain the same equation of motion (2.2) with (2.3) unchanged, but with the transformed Hamilton operator

$$H/\hbar = \Delta\sigma_z/2 + g(a\sigma^+ + a^\dagger\sigma^-) , \qquad (2.5)$$

where $\Delta = \omega_a - \omega_c$ is the detuning.

Introducing matrix elements with respect to the two atomic states $|\uparrow\rangle, |\downarrow\rangle$ (denoting $\langle\uparrow|\rho|\uparrow\rangle$ by $\rho_{\uparrow\uparrow}$, etc.) the equations of motion read

$$\begin{aligned} \dot{\rho}_{\uparrow\uparrow} &= ig(\rho_{\uparrow\downarrow}a^\dagger - a\rho_{\downarrow\uparrow}) + \kappa L_{\rm ir}(\rho_{\uparrow\uparrow}) , \\ \dot{\rho}_{\downarrow\downarrow} &= ig(\rho_{\downarrow\uparrow}a - a^\dagger\rho_{\uparrow\downarrow}) + \kappa L_{\rm ir}(\rho_{\downarrow\downarrow}) , \\ \dot{\rho}_{\uparrow\downarrow} &= -i\Delta\rho_{\uparrow\downarrow} + ig(\rho_{\uparrow\uparrow}a - a\rho_{\downarrow\downarrow}) + \kappa L_{\rm ir}(\rho_{\uparrow\downarrow}) , \\ \dot{\rho}_{\downarrow\uparrow} &= i\Delta\rho_{\downarrow\uparrow} + ig(\rho_{\downarrow\downarrow}a^\dagger - a^\dagger\rho_{\uparrow\uparrow}) + \kappa L_{\rm ir}(\rho_{\downarrow\uparrow}) . \end{aligned} \qquad (2.6)$$

Notice that the atomic matrix elements are still operators with respect to the light mode.

Instead of the four matrix elements $\rho_{\uparrow\uparrow}, \rho_{\uparrow\downarrow}, \ldots$ we use the following six combinations of the matrix elements:

$$\begin{aligned} \rho_1 &= \rho_{\uparrow\uparrow} + \rho_{\downarrow\downarrow} , \\ \rho_2 &= \rho_{\uparrow\uparrow} - \rho_{\downarrow\downarrow} , \\ \rho_3 &= i(a\rho_{\downarrow\uparrow} - \rho_{\uparrow\downarrow}a^\dagger)/2 , \\ \rho_4 &= i(\rho_{\downarrow\uparrow}a - a^\dagger\rho_{\uparrow\downarrow})/2 , \\ \rho_5 &= (a\rho_{\downarrow\uparrow} + \rho_{\uparrow\downarrow}a^\dagger)/2 , \\ \rho_6 &= (\rho_{\downarrow\uparrow}a + a^\dagger\rho_{\uparrow\downarrow})/2 . \end{aligned} \qquad (2.7)$$

These combinations are Hermitian operators with respect to the light field. From the equations of motion of the four matrix elements we obtain the following closed system of equations of motion for the combinations $\rho_1, \ldots, \rho_6$:

$$
\begin{aligned}
\dot{\rho}_1 &= -2g\rho_3 + 2g\rho_4 + \kappa L_{\mathrm{ir}}(\rho_1) \,, \\
\dot{\rho}_2 &= -2g\rho_3 - 2g\rho_4 + \kappa L_{\mathrm{ir}}(\rho_2) \,, \\
\dot{\rho}_3 &= -\Delta\rho_5 + (g/4)(\rho_1 aa^\dagger + aa^\dagger\rho_1 - 2a\rho_1 a^\dagger \\
&\qquad + \rho_2 aa^\dagger + aa^\dagger\rho_2 + 2a\rho_2 a^\dagger) \\
&\quad + \kappa[L_{\mathrm{ir}}(\rho_3) - (2n_{\mathrm{th}}+1)\rho_3 + 2n_{\mathrm{th}}\rho_4] \,, \\
\dot{\rho}_4 &= -\Delta\rho_6 + (g/4)(2a^\dagger\rho_1 a - a^\dagger a\rho_1 - \rho_1 a^\dagger a \\
&\qquad + 2a^\dagger\rho_2 a + a^\dagger a\rho_2 + \rho_2 a^\dagger a) \\
&\quad + \kappa[L_{\mathrm{ir}}(\rho_4) + (2n_{\mathrm{th}}+1)\rho_4 - 2(n_{\mathrm{th}}+1)\rho_3] \,, \\
\dot{\rho}_5 &= \Delta\rho_3 + i(g/4)(\rho_1 aa^\dagger - aa^\dagger\rho_1 + \rho_2 aa^\dagger - aa^\dagger\rho_2) \\
&\quad + \kappa[L_{\mathrm{ir}}(\rho_5) - (2n_{\mathrm{th}}+1)\rho_5 + 2n_{\mathrm{th}}\rho_6] \,, \\
\dot{\rho}_6 &= \Delta\rho_4 + i(g/4)(\rho_1 a^\dagger a - a^\dagger a\rho_1 - \rho_2 a^\dagger a + a^\dagger a\rho_2) \\
&\quad + \kappa[L_{\mathrm{ir}}(\rho_6) + (2n_{\mathrm{th}}+1)\rho_6 - 2(n_{\mathrm{th}}+1)\rho_5] \,.
\end{aligned}
\tag{2.8}
$$

As shown in Sec. III, the equations of motion for the expansion coefficients of the quasiprobability distribution following from (2.8) are tridiagonally coupled in only one index whereas the equations of motion for the expansion coefficients of the four matrix elements are tridiagonally coupled in both indices. Therefore the equations of motion for the expansion coefficients are much easier to solve for the six combinations than for the four matrix elements. The reason why (2.8) leads to a more simple coupling than (2.6) is the following. In (2.8) the creation and annihilation operators only occur bilinearly, i.e., in the form $\rho a^\dagger a$, $a\rho a^\dagger, \ldots$, whereas in (2.6), in addition to these bilinear terms occurring in L_{ir}, the creation and annihilation operators occur also linearly, i.e., in the form $\rho a^\dagger$, ρa, ... In the equation for the quasiprobability distributions in Sec. III these linear terms lead to terms which contain $\exp(\pm i\phi)$, whereas the bilinear terms do not contain any explicit dependence on ϕ (though derivatives with respect to ϕ do occur). The terms $\exp(\pm i\phi)$ lead to a coupling of the coefficients also in the other index.

The Fock representation of (2.8) is also much simpler. Denoting the matrix elements in the Fock representation by $\rho_{n,m}$ the terms $a\rho a^\dagger$ and $a^\dagger\rho a$ give rise to terms proportional to $\rho_{n+1,m+1}$ and $\rho_{n-1,m-1}$. Thus the difference $n-m$ between the two indices is not changed. Introducing the sum and the difference of the two indices as new indices leads again to a coupling in only one index.

If we are interested in the properties of the light field, we have to perform a trace with respect to the atom (A), i.e.,

$$
\mathrm{Tr}_A(\rho) = \rho_{\uparrow\uparrow} + \rho_{\downarrow\downarrow} = \rho_1 \,. \tag{2.9}
$$

If we are interested in the inversion D of the atom, we have to perform a trace with respect to the atom (A) and the field (F) according to

$$
D = \mathrm{Tr}_{AF}(\sigma_z\rho) = \mathrm{Tr}_F(\rho_{\uparrow\uparrow} - \rho_{\downarrow\downarrow}) = \mathrm{Tr}_F(\rho_2) \,. \tag{2.10}
$$

Without detuning ($\Delta = 0$) ρ_5 and ρ_6 do not enter into the first four equations in (2.8). Because we are mainly interested in the field (ρ_1) and in the inversion (ρ_2) we just need to solve the first four equations in (2.8) for vanishing detuning.

A. Initial values

In this paper we assume that initially the atom is in its upper state and that the cavity mode is in the coherent state $|\alpha_0\rangle$. (For the sake of simplicity we further assume that α_0 is real. If α_0 is complex we can always transform to a real α_0 by a suitable rotation.) Therefore the initial condition for the density operator of the system reads

$$
\rho(0) = |\uparrow\rangle\langle\uparrow| \otimes |\alpha_0\rangle\langle\alpha_0| \,. \tag{2.11}
$$

The initial conditions for the six combinations $\rho_1, \ldots, \rho_6$ then take the form

$$
\begin{aligned}
&\rho_1(0) = \rho_2(0) = |\alpha_0\rangle\langle\alpha_0| \,, \\
&\rho_3(0) = \rho_4(0) = \rho_5(0) = \rho_6(0) = 0 \,.
\end{aligned}
\tag{2.12}
$$

B. Stationary solution

For a finite cavity damping constant κ and a finite coupling constant g the solutions of (2.8) always reach the stationary solution for $t \to \infty$,

$$
\begin{aligned}
\rho_1(\infty) &= \frac{1}{1+n_{\mathrm{th}}} \left(\frac{n_{\mathrm{th}}}{1+n_{\mathrm{th}}} \right)^{a^\dagger a} \\
&= (1-e^{-r}) \exp(-ra^\dagger a) \,, \\
\rho_2(\infty) &= -[1/(1+2n_{\mathrm{th}})]\rho_1(\infty) \\
&= -\tanh(r/2)\rho_1(\infty) \,, \\
\rho_i(\infty) &= 0 \quad \text{for} \quad i = 3, \ldots, 6 \,,
\end{aligned}
\tag{2.13}
$$

where r is the ratio

$$
r = \hbar\omega_c/(kT) \,. \tag{2.14}
$$

In the stationary state the inversion (2.10) is given by

$$
\begin{aligned}
D(\infty) &= -1/(1+2n_{\mathrm{th}}) = -\tanh[\hbar\omega_c/(2kT)] \\
&\approx -\tanh[\hbar\omega_a/(2kT)] \,.
\end{aligned}
\tag{2.15}
$$

In the rotating-wave approximation the damping constant, the detuning, and the coupling constant must be small compared to the frequency, i.e.,

$$
\kappa, \ |\Delta|, \ g \ll \omega_c \approx \omega_a \,. \tag{2.16}
$$

Neglecting the coupling in (2.1), the stationary solution in the original and in the interaction picture is thus given by the thermal solution

$$
\rho = \exp[-H_0/(kT)]/\mathrm{Tr}_{AF}\{\exp[-H_0/(kT)]\} \,, \tag{2.17}
$$

with H_0 given by $\hbar\omega_c a^\dagger a + \hbar\omega_a\sigma_z/2$.

III. QUASIPROBABILITY DISTRIBUTIONS

As quasiprobability distributions we use the s-parametrized quasiprobability distributions $W(\alpha, s)$ introduced by Cahill and Glauber.[18] These distributions are c-number representations of the density operator, which contain the usual quasiprobability functions (P, Wigner, Q function) as special cases. In the present case we use for each of the six $\rho_i(t)$ the distributions $W_i(\alpha, s; t)$. They may be defined as Fourier transforms of the characteristic functions (our definitions deviate from those of Ref. 18 by a factor of $1/\pi$)

$$\chi_i(\xi, s; t) = \mathrm{Tr}_F[\exp(\xi a^\dagger - \xi^* a + s|\xi|^2/2)\rho_i(t)] , \quad (3.1)$$

i.e.,

$$W_i(\alpha, s; t) = \frac{1}{\pi^2} \int \chi_i(\xi, s; t) \exp(\alpha\xi^* - \alpha^*\xi) d^2\xi . \quad (3.2)$$

With these distribution functions, s-ordered products $\langle\{(a^\dagger)^n a^m\}_s\rangle_i$ can be obtained by proper integration with weight $W_i(\alpha, s; t)$ in the complex α plane according to

$$\langle\{(a^\dagger)^n a^m\}_s\rangle_i = \mathrm{Tr}_F[\{(a^\dagger)^n a^m\}_s \rho_i(t)] = \int (\alpha^*)^n \alpha^m W_i(\alpha, s; t)\, d^2\alpha . \quad (3.3)$$

For the special choices of the parameter $s = 1, 0, -1$, the s-ordered products are the normal, symmetric, and antinormal ordered products and the quasiprobability distributions are the P, Wigner, and Q functions. (For a definition of s-ordered products for arbitrary s, see Ref. 18.)

The system of equations of motion (2.8) transforms into a system of partial-differential equations for the distributions W_i. Applying the relations in Table I of Ref. 24 twice, this system is obtained by a simple though lengthy calculation. For further considerations it is advantageous to use intensity I and phase ϕ variables defined by

$$\alpha = \sqrt{I}\, \exp(i\phi) . \quad (3.4)$$

Because of

$$\frac{\partial}{\partial\alpha} = \left(\frac{\partial}{\partial I} - \frac{i}{2I}\frac{\partial}{\partial\phi}\right)\sqrt{I}\, e^{-i\phi} = \sqrt{I}\, e^{-i\phi}\left(\frac{\partial}{\partial I} - \frac{i}{2I}\frac{\partial}{\partial\phi}\right) \quad (3.5)$$

and its complex-conjugate counterpart, the transformation to intensity and phase variables is easily achieved. In this way we obtain from (2.8) the following system for the quasiprobabilities $W_i(I, \phi, s; t)$:

$$\begin{aligned}
\dot{W}_1 &= -2gW_3 + 2gW_4 + \kappa\left(2\frac{\partial}{\partial I}I + (2n_{\mathrm{th}} + 1 - s)\Delta_2\right) W_1 , \\
\dot{W}_2 &= -2gW_3 - 2gW_4 + \kappa\left(2\frac{\partial}{\partial I}I + (2n_{\mathrm{th}} + 1 - s)\Delta_2\right) W_2 , \\
\dot{W}_3 &= -\Delta W_5 + \frac{g}{2}\left(1 - \frac{\partial}{\partial I}I + \frac{s-1}{2}\Delta_2\right) W_1 + \frac{g}{2}\left(2I + s + (1-2s)\frac{\partial}{\partial I}I + \frac{s(s-1)}{2}\Delta_2\right) W_2 \\
&\quad + \kappa\left[\left(2\frac{\partial}{\partial I}I - (2n_{\mathrm{th}} + 1) + (2n_{\mathrm{th}} + 1 - s)\Delta_2\right) W_3 + 2n_{\mathrm{th}} W_4\right] , \\
\dot{W}_4 &= -\Delta W_6 + \frac{g}{2}\left(1 - \frac{\partial}{\partial I}I + \frac{s+1}{2}\Delta_2\right) W_1 + \frac{g}{2}\left(2I + s - (1+2s)\frac{\partial}{\partial I}I + \frac{s(s+1)}{2}\Delta_2\right) W_2 \\
&\quad + \kappa\left[\left(2\frac{\partial}{\partial I}I + (2n_{\mathrm{th}} + 1) + (2n_{\mathrm{th}} + 1 - s)\Delta_2\right) W_4 - 2(n_{\mathrm{th}} + 1) W_3\right] , \\
\dot{W}_5 &= \Delta W_3 + \frac{g}{4}\left(\frac{\partial W_1}{\partial\phi} + \frac{\partial W_2}{\partial\phi}\right) + \kappa\left[\left(2\frac{\partial}{\partial I}I - (2n_{\mathrm{th}} + 1) + (2n_{\mathrm{th}} + 1 - s)\Delta_2\right) W_5 + 2n_{\mathrm{th}} W_6\right] , \\
\dot{W}_6 &= \Delta W_4 + \frac{g}{4}\left(\frac{\partial W_1}{\partial\phi} - \frac{\partial W_2}{\partial\phi}\right) + \kappa\left[\left(2\frac{\partial}{\partial I}I + (2n_{\mathrm{th}} + 1) + (2n_{\mathrm{th}} + 1 - s)\Delta_2\right) W_6 - 2(n_{\mathrm{th}} + 1) W_5\right] .
\end{aligned} \quad (3.6)$$

Here Δ_2 is an abbreviation for

$$\Delta_2 = \frac{\partial}{\partial I} I \frac{\partial}{\partial I} + \frac{1}{4I}\frac{\partial^2}{\partial\phi^2} , \quad (3.7)$$

which is one-fourth of the two-dimensional Laplace operator. Because of (2.9), the Cahill-Glauber distribution for the light field is given by $W_1(I, \phi, s; t)$. In the intensity and phase variables the integration with respect to α has to be replaced according to

$$\int \cdots d^2\alpha \Rightarrow \tfrac{1}{2}\int_0^\infty \int_0^{2\pi} \cdots dI\, d\phi . \quad (3.8)$$

Therefore the inversion (2.10) now takes the form

$$D(t) = \tfrac{1}{2}\int_0^\infty \int_0^{2\pi} W_2(I, \phi, s; t)\, dI\, d\phi . \quad (3.9)$$

The initial conditions for the distributions $W_i(\alpha, s; t)$ are easily obtained by inserting (2.12) into (3.1) and evaluating the integral in (3.2). At t=0 the W_1, W_2 are shifted Gaussians in the α variable. With $\alpha_0 = \sqrt{I_0}$ real, the W_i read in intensity and phase variables for t=0

$$W_1(I,\phi,s;0) = W_2(I,\phi,s;0) = \frac{2}{\pi(1-s)}\exp\left(-\frac{2}{(1-s)}(I-2\sqrt{II_0}\cos\phi+I_0)\right),$$
$$W_i(I,\phi,s;0)=0 \quad \text{for} \quad i=3,\ldots,6 . \tag{3.10}$$

For the stationary distribution W_1 we obtain from (2.13)

$$W_1(I,\phi,s;\infty) = \frac{2}{\pi(1-s+2n_{\text{th}})}\exp\left(-\frac{2I}{1-s+2n_{\text{th}}}\right) . \tag{3.11}$$

IV. EXPANSIONS OF THE DISTRIBUTION FUNCTIONS

In order to handle the coupled partial-differential equations (3.6) we expand the distributions W_i into two complete sets. Because the $W_i(I,\phi,s;t)$ are periodic in ϕ and only defined for $I \geq 0$ we use a Fourier series with respect to ϕ and Laguerre functions with respect to I, i.e.,

$$W_i(I,\phi,s;t) = \sum_{m=0}^{\infty}\sum_{n=-\infty}^{\infty} c_{n,m}^{(i)}(t)e^{in\phi}(I/\tilde{I})^{|n|/2} \times L_m^{(|n|)}(I/\tilde{I})\exp(-I/\tilde{I}) . \tag{4.1}$$

Here $L_m^{(|n|)}$ are the generalized Laguerre polynomials and $\tilde{I}$ is an arbitrary scaling intensity, which is chosen such that good numerical convergence is achieved. Inserting the expansion (4.1) into (3.6) and using the recurrence relations and orthogonality relations for the generalized Laguerre polynominals,[25] we obtain the following equation of motion for the expansion coefficients ($m \geq 0$, coefficients with a negative index m formally occurring for $m=0$ can be omitted because of the prefactor m):

$$\begin{aligned}
\dot{c}_{n,m}^{(1)} &= -2gc_{n,m}^{(3)} + 2gc_{n,m}^{(4)} + \kappa[amc_{n,m-1}^{(1)} - (2m+|n|)c_{n,m}^{(1)}] ,\\
\dot{c}_{n,m}^{(2)} &= -2gc_{n,m}^{(3)} - 2gc_{n,m}^{(4)} + \kappa[amc_{n,m-1}^{(2)} - (2m+|n|)c_{n,m}^{(2)}] ,\\
\dot{c}_{n,m}^{(3)} &= -\Delta c_{n,m}^{(5)} + g\{(1+m+|n|/2)c_{n,m}^{(1)} - m[1-(1-s)/(2\tilde{I})]c_{n,m-1}^{(1)}\\
&\qquad + [2\tilde{I}(2m+1+|n|)+s-(1-2s)(m+|n|/2)]c_{n,m}^{(2)} - b^{+}mc_{n,m-1}^{(2)} - 2\tilde{I}(m+1+|n|)c_{n,m+1}^{(2)}\}/2\\
&\quad + \kappa[amc_{n,m-1}^{(3)} - (2m+|n|+2n_{\text{th}}+1)c_{n,m}^{(3)} + 2n_{\text{th}}c_{n,m}^{(4)}] ,\\
\dot{c}_{n,m}^{(4)} &= -\Delta c_{n,m}^{(6)} + g\{(1+m+|n|/2)c_{n,m}^{(1)} - m[1+(1+s)/(2\tilde{I})]c_{n,m-1}^{(1)}\\
&\qquad + [2\tilde{I}(2m+1+|n|)+s+(1+2s)(m+|n|/2)]c_{n,m}^{(2)} - b^{-}mc_{n,m-1}^{(2)} - 2\tilde{I}(m+1+|n|)c_{n,m+1}^{(2)}\}/2\\
&\quad + \kappa[amc_{n,m-1}^{(4)} - (2m+|n|-2n_{\text{th}}-1)c_{n,m}^{(4)} - 2(n_{\text{th}}+1)c_{n,m}^{(3)}] ,\\
\dot{c}_{n,m}^{(5)} &= \Delta c_{n,m}^{(3)} + ign(c_{n,m}^{(1)} + c_{n,m}^{(2)})/4 + \kappa[amc_{n,m-1}^{(5)} - (2m+|n|+2n_{\text{th}}+1)c_{n,m}^{(5)} + 2n_{\text{th}}c_{n,m}^{(6)}] ,\\
\dot{c}_{n,m}^{(6)} &= \Delta c_{n,m}^{(4)} + ign(c_{n,m}^{(1)} - c_{n,m}^{(2)})/4 + \kappa[amc_{n,m-1}^{(6)} - (2m+|n|-2n_{\text{th}}-1)c_{n,m}^{(6)} - 2(n_{\text{th}}+1)c_{n,m}^{(5)}] .
\end{aligned} \tag{4.2}$$

The constants a and $b^{\pm}$ are defined by

$$a = 2-(2n_{\text{th}}+1-s)/\tilde{I} ,$$
$$b^{\pm} = 2\tilde{I}+2s\mp 1+s(s\mp 1)/(2\tilde{I}) . \tag{4.3}$$

By introducing the vector

$$\mathbf{c}_m = \begin{pmatrix} c_{n,m}^{(1)} \\ c_{n,m}^{(2)} \\ \vdots \\ c_{n,m}^{(6)} \end{pmatrix} \tag{4.4}$$

the system (4.2) can be cast into the tridiagonal vector recurrence relation

$$\dot{\mathbf{c}}_m = \mathbf{Q}_m^{-}\mathbf{c}_{m-1} + \mathbf{Q}_m\mathbf{c}_m + \mathbf{Q}_m^{+}\mathbf{c}_{m+1} , \tag{4.5}$$

with matrices $\mathbf{Q}_m^{\pm}$ and $\mathbf{Q}_m$ following from (4.2). In the system (4.2) of ordinary differential equations or, equivalently, in the tridiagonal vector recurrence relation (4.5) a tridiagonal coupling occurs in only the second index m, the first index n appears only as a parameter. Because of this simple coupling, it is quite easy to solve (4.2) or (4.5). If we apply the same method to the four matrix elements $\rho_{\uparrow\uparrow}$, $\rho_{\uparrow\downarrow}$, $\rho_{\downarrow\uparrow}$, $\rho_{\downarrow\downarrow}$ we obtain, in addition to the tridiagonal coupling in the second index m, also a tridiagonal coupling in the first index n.

A. Initial values

In order to obtain the initial values for the expansion coefficients $c_{n,m}^{(i)}$ we first expand the phase part of the initial distributions W_1, W_2 in (3.10) into modified Bessel functions I_n according to

$$\exp[z\cos(\phi)] = \sum_{n=-\infty}^{\infty} I_n(z)\exp(in\phi) . \tag{4.6}$$

Comparing the $\exp(in\phi)$ terms of (3.10) with the corresponding terms in (4.1) we have for $i = 1, 2$

$$\frac{2}{\pi(1-s)} \exp\left(-\frac{2(I+I_0)}{1-s}\right) I_n\left(\frac{4\sqrt{II_0}}{1-s}\right)$$

$$= \sum_{m=0}^{\infty} c_{n,m}^{(i)}(0)(I/\tilde{I})^{|n|/2} L_m^{(|n|)}(I/\tilde{I}) \exp(-I/\tilde{I}) \,. \tag{4.7}$$

Multiplying this equation by $(I/\tilde{I})^{|n|/2} L_{m'}^{(|n|)}(I/\tilde{I})$, integrating the resulting equation over I, using the orthogonality relation for the Laguerre functions and Ref. 26 we thus obtain

$$c_{n,m}^{(1)}(0) = c_{n,m}^{(2)}(0)$$
$$= \frac{m!}{\pi\tilde{I}(m+|n|)!}\left(\frac{I_0}{\tilde{I}}\right)^{|n|/2}\left(\frac{2\tilde{I}+s-1}{2\tilde{I}}\right)^m$$
$$\times L_m^{(|n|)}\left(\frac{2I_0}{2\tilde{I}+s-1}\right) ,$$
$$c_{n,m}^{(i)}(0) = 0 \quad \text{for} \quad i = 3, \ldots, 6 \,. \tag{4.8}$$

B. Expectation values

Expectation values are usually expressed by some of the first few coefficients. For instance, the averaged intensity, the averaged complex amplitude, and the inversion are given by

$$\bar{I}(t) = \langle I \rangle = \mathrm{Tr}_F[a^\dagger a \rho_1(t)]$$
$$= \tfrac{1}{2}\int_0^\infty \int_0^{2\pi} I\, W_1(I,\phi,s;t)\, dI\, d\phi - (1-s)/2$$
$$= \pi\tilde{I}^2 [c_{0,0}^{(1)}(t) - c_{0,1}^{(1)}(t)] - (1-s)/2 \,, \tag{4.9}$$

$$\bar{a}(t) = \mathrm{Tr}_F[a\rho_1(t)]$$
$$= \tfrac{1}{2}\int_0^\infty \int_0^{2\pi} \sqrt{I}\, e^{i\phi} W_1(I,\phi,s;t)\, dI\, d\phi$$
$$= \pi\tilde{I}^{3/2} c_{-1,0}^{(1)}(t) \,, \tag{4.10}$$

$$D(t) = \langle \sigma_z \rangle = \mathrm{Tr}_F[\rho_2(t)]$$
$$= \tfrac{1}{2}\int_0^\infty \int_0^{2\pi} W_2(I,\phi,s;t)\, dI\, d\phi$$
$$= \pi\tilde{I}\, c_{0,0}^{(2)}(t) \,. \tag{4.11}$$

(To derive (4.9) we have used the relation $a^\dagger a = \{a^\dagger a\}_s - (1-s)/2$ for the s-ordered product, we have expressed I by $\tilde{I}\,[L_0^{(0)}(I/\tilde{I}) - L_1^{(0)}(I/\tilde{I})]$ and applied the orthogonality relations for the Laguerre polynomials.) Thus, in order to obtain $\bar{I}(t)$ and $D(t)$, we need to solve (4.2) only for n=0, to obtain $\bar{a}(t)$ we need to solve (4.2) only for $n = -1$.

C. Numerical method

The system (4.2) or, equivalently, the tridiagonal vector recurrence relation (4.5) with given initial conditions such as (4.8) can be integrated by any numerical method for solving systems of ordinary differential equations. For these numerical methods the infinite system has to be truncated. The truncation indices M and $\pm N$ at which the infinite sums in (4.1) are truncated must be chosen such that a further increase of M and N does not change the results within a given accuracy. The truncation indices increase for increasing initial photon intensities. For I_0=10 we get results with an accuracy sufficient for the plots with M=100 and N=20. Because the expansion coefficients are not coupled in the first index n, we can integrate the system for each n separately. As already mentioned the ρ_i in (2.5) are Hermitian operators. Therefore the W_i are always real, leading for the expansion coefficients in (4.1) to the relation

$$c_{-n,m}^{(i)}(t) = [c_{n,m}^{(i)}(t)]^* \,. \tag{4.12}$$

Thus we generally need to integrate the system (4.2) only for $n \geq 0$.

For the integration we have used a fourth-order Runge-Kutta method.[27] With the Runge-Kutta method the next time step follows through some intermediate steps explicitly from the previous one. Using the vector notation we thus obtain the coefficients $\mathbf{c}_m(t+h)$ at the later time $t+h$ from the previous coefficients $\mathbf{c}_m(t)$ starting with m=0 and proceeding to $m = M$. This procedure has the advantage that the previous coefficients can be overwritten. Therefore, besides 6×12 coefficients needed for the intermediate steps, we only need to store $6 \times M$ complex numbers. Even for M=100 a PC can easily handle these numbers and therefore the integration can be performed on a PC. The value of the time step h has to be chosen in such a way that a further decrease does not change the final result. If h is too large, numerical instabilities usually occur.

As explained in Chap. 9 of Ref. 28, the eigenvalues as well as the Laplace transform of the Green's function of the tridiagonal vector recurrence relation (4.5) can be obtained in terms of matrix continued fractions. By numerically inverting the Laplace transform of each of the coefficients, the solution of (4.5) with the initial values (4.8) may in principle be obtained. If only a few coefficients as in (4.9)–(4.11) enter, this method is feasible. For calculating the quasiprobability distribution W_1, where all the $N \times M$ Laplace transforms of the coefficients $c_{n,m}^{(1)}$ need to be inverted, this procedure becomes too time consuming. Therefore the direct integration as described above is much more suitable for calculating the quasiprobability distribution.

V. RESULTS

We first discuss the Q function for vanishing damping. As explained in Appendix A without damping the

Q function is easily evaluated. The method developed in Secs. II–IV also works for vanishing damping up to $I_0 \approx 30$. For the initial condition (2.11) the contour lines of the Q function are shown in Fig. 1 for several times. In addition, the inversion $D(t)$ as a function of time is also shown in this figure. As seen, the initial distribution of the Q function is a single Gaussian distribution centered around α_0. The most striking result is that in the course of time the initial one-peaked function splits into two peaks, which counterrotate on the circle $|\alpha| \approx \alpha_0$ till they collide at $\phi = \pi$. Then they split again, collide at $\phi = 0$ and so on. Near the initial time the inversion shows pronounced Rabi oscillations. When the distribution has split into two peaks the Rabi oscillations collapse. At the collision of the peaks a revival of the Rabi oscillations is observed. The details of the initial splitting are shown in Fig. 2. At first the maximum shifts a little bit to a larger value because the inversion goes down and the light intensity is thus increased. Next the inverse effect occurs, i.e., the peak is shifted to lower intensities. After a couple of oscillations the peak is finally split into two peaks. A similar oscillation of the intensity is observed when the peaks collide at $\phi = \pi$.

In the course of time the width of the peaks in the ϕ direction increases monotonously. If it has spread along the circle $|\alpha| \approx \alpha_0$, the collapse of the inversion ceases to exist. Finally for very large times we obtain the nearly annular but coarse structure, see Fig. 3.

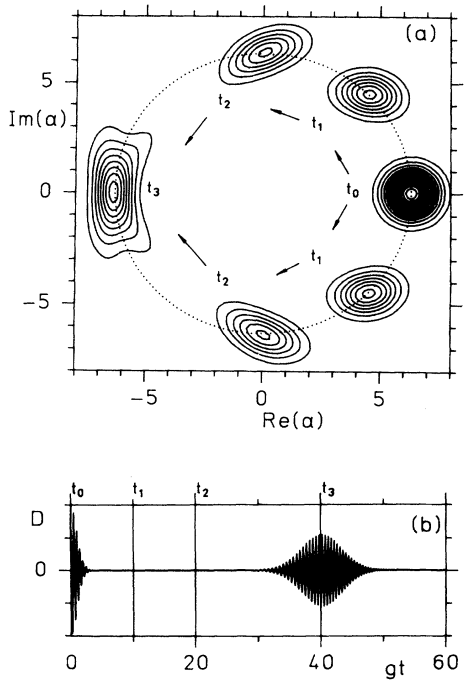

FIG. 1. (a) Contour lines of $Q(\alpha, t) = W_1(\alpha, -1, t)$ in the complex α plane without detuning $\Delta = 0$ and damping $\kappa = 0$ for $I_0 = 40$ at the times $gt_0 = 0$, $gt_1 = 10$, $gt_2 = 20$, $gt_3 = 40$. (b) The inversion $D(t)$ as a function of gt for the same parameters. The times t_0, t_1, t_2, t_3 are indicated by the vertical bars.

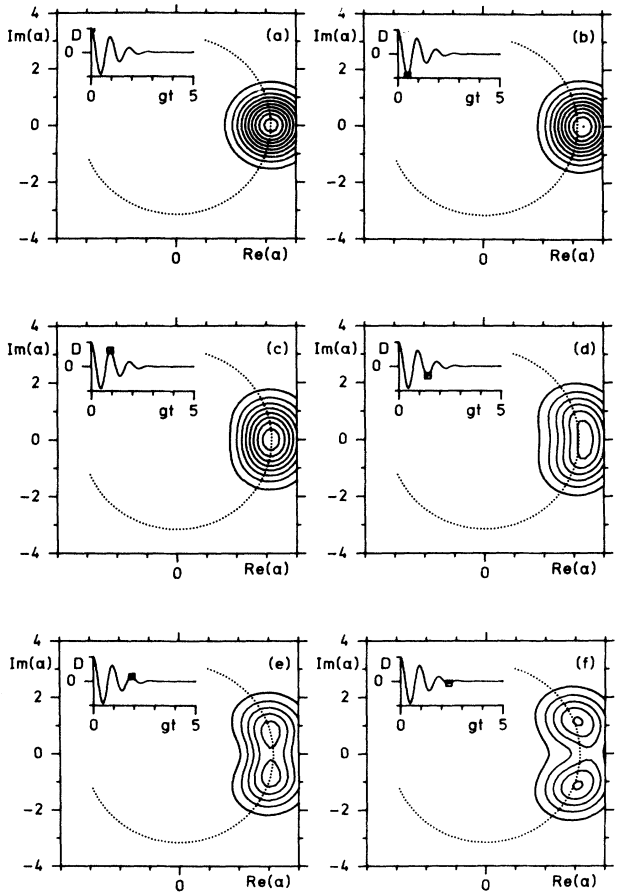

FIG. 2. Initial splitting of $Q(\alpha, t) = W_1(\alpha, -1, t)$ without detuning $\Delta = 0$ and damping $\kappa = 0$ for $I_0 = 10$. Shown are those times which correspond to the extrema of the inversion, see the black squares in the inset.

With a small damping constant the two peaks first counterrotate and at the same time move towards the origin, or in other words, they spiral in a countermotion towards the origin, see Fig. 4. As was the case without damping, the width in the ϕ direction becomes broader.

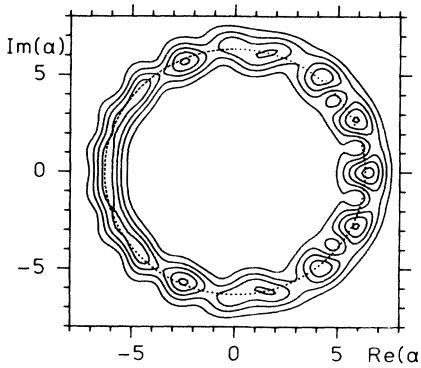

FIG. 3. Contour lines of $Q(\alpha, t) = W_1(\alpha, -1, t)$ $= 0.004, 0.008, \ldots$ for the large time $gt = 430$ and for $I_0 = 40$, $\Delta = \kappa = 0$.

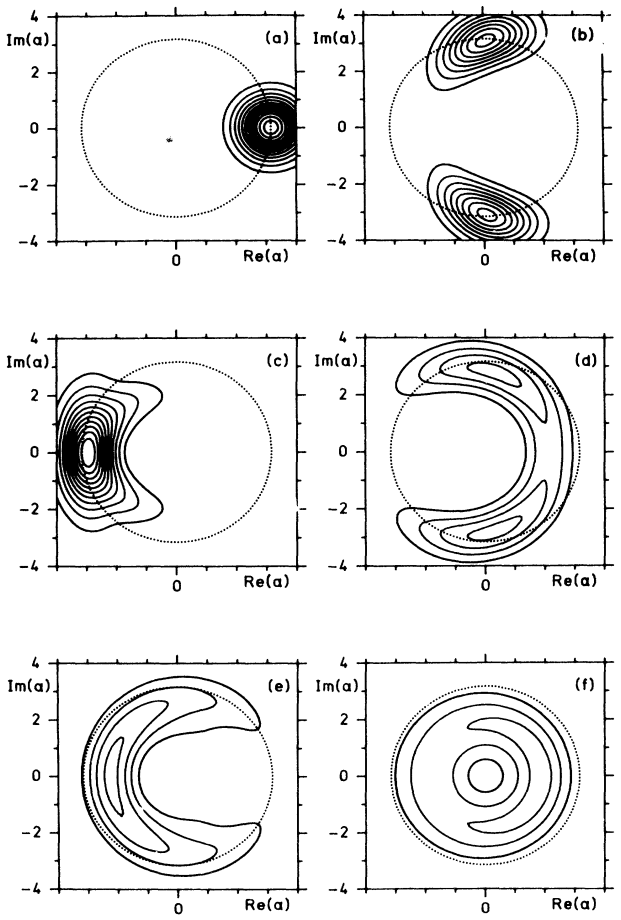

FIG. 4. The contour lines of $Q(\alpha,t) = W_1(\alpha, s=-1, t)$ in the complex α plane for the times (a) $gt = 0$, (b) $gt = 10$, (c) $gt = 20$, (d) $gt = 30$, (e) $gt = 50$, (f) $gt = 100$. The parameters are $\kappa/g = 0.005$, $\Delta = 0, n_{\rm th} = 0, \alpha_0^2 = I_0 = 10$. The circle $|\alpha| = \alpha_0$ is also dotted in.

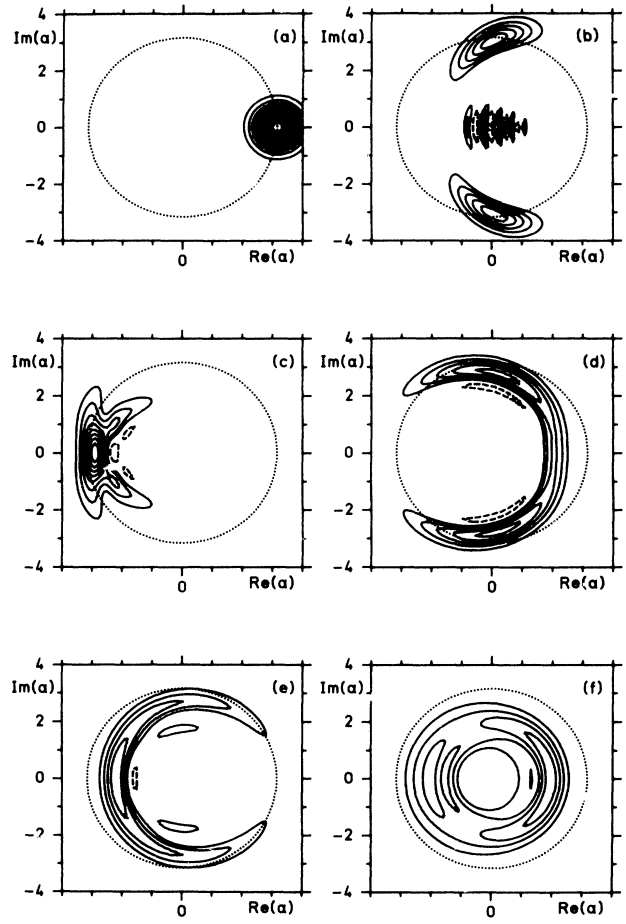

FIG. 5. The contour lines of the Wigner function $W_1(\alpha, s=0, t)$ in the complex α plane for the times and the same parameters as in Fig. 4. Negative values are shown by dashed lines. The circle $|\alpha| = \alpha_0$ is also dotted in.

In contrast to the case without damping, the structure becomes smooth and nearly independent of ϕ for larger times, see Fig. 4(f). Near the origin the distribution still has a minimum for this time. Finally this minimum becomes a maximum in the course of time and the distribution shrinks to the stationary distribution (3.11).

The Wigner distribution is shown in Fig. 5 for the same parameters as in Fig. 4. The main differences between the Wigner and the Q functions are that the Wigner function is smaller than the Q function and that rapid variations with negative values appear near the real axis. They are similar to those found for the superposition of two coherent states.[29]

In Fig. 6 the inversion and the mean intensity are shown as a function of time. For vanishing damping

$$\bar{I}(t) + D(t)/2 = I_0 + 1/2 \tag{5.1}$$

is a constant of motion, i.e., oscillations of the mean intensity always lead to oscillations of the inversion. Though for finite damping (5.1) no longer holds exactly, oscillations of the mean intensity still lead to oscillations of the inversion. The main feature of the mean intensity is, of course, the decay of the intensity. Disregarding the small rapid oscillations this decay is approximately given by

$$\bar{I}(t) = (I_0 + 1/2)\exp(-2\kappa t)\,. \tag{5.2}$$

It is worth noticing that the inversion D remains nearly zero up to those times, where the light intensity is of the order 1. Then the inversion approaches its stationary value (2.15). The mean complex amplitude is shown in Fig. 7. The real part of the complex field shows a damped oscillation as a function of gt. As seen for finite $n_{\rm th}$ the damping increases. The minimal eigenvalue of the variance matrix V_{rr}, V_{ri}, ... of the quadrature phases $a_r = (a + a^\dagger)/2$ and $a_i = (a - a^\dagger)/(2i)$ is shown in Fig. 8. As already said in Ref. 22 each peak of the Q function already shows squeezing, see Appendix A. Usually the quadrature phase is calculated from the density operator. This is equivalent to calculating the matrix of the

quadrature phase from the total Q function. Then we can get squeezing only for those times, where the two peaks collide. As seen in Fig. 8 this squeezing ceases to exist already for a larger number of thermal photons as well as for a larger cavity damping. It should be noted that these averaged quantities do not depend on the parameter s used for representing the density operators. As already remarked by Kuklinski and Madajczyk,[16] by choosing an appreciable detuning, squeezing is increased. This effect is easily seen by comparing Fig. 8(a) with Fig. 8(b).

In the figures of the quasiprobability distributions discussed so far we have not included detuning. In Fig. 9 the Q function is shown for an appreciable detuning. As is

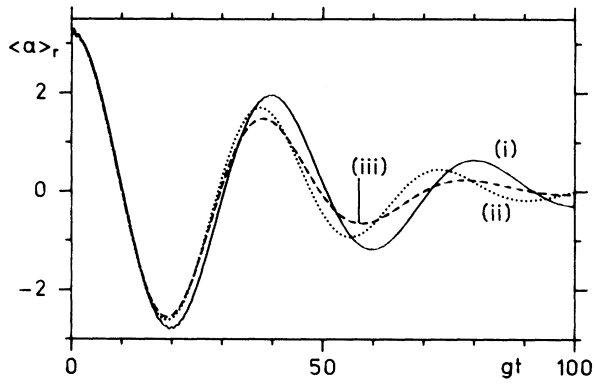

FIG. 7. The real part of the average complex amplitude $\bar{a}(t) = \langle a \rangle$ as a function of gt for the parameters (i) $\kappa/g = 0.002$, $n_{\rm th} = 0$, (ii) $\kappa/g = 0.005$, $n_{\rm th} = 0$, (iii) $\kappa/g = 0.005$, $n_{\rm th} = 1.5$ and for $\Delta = 0$, $\alpha_0^2 = I_0 = 10$. [For vanishing detuning the imaginary part is identical to zero for the initial conditions (2.11) with real α_0.]

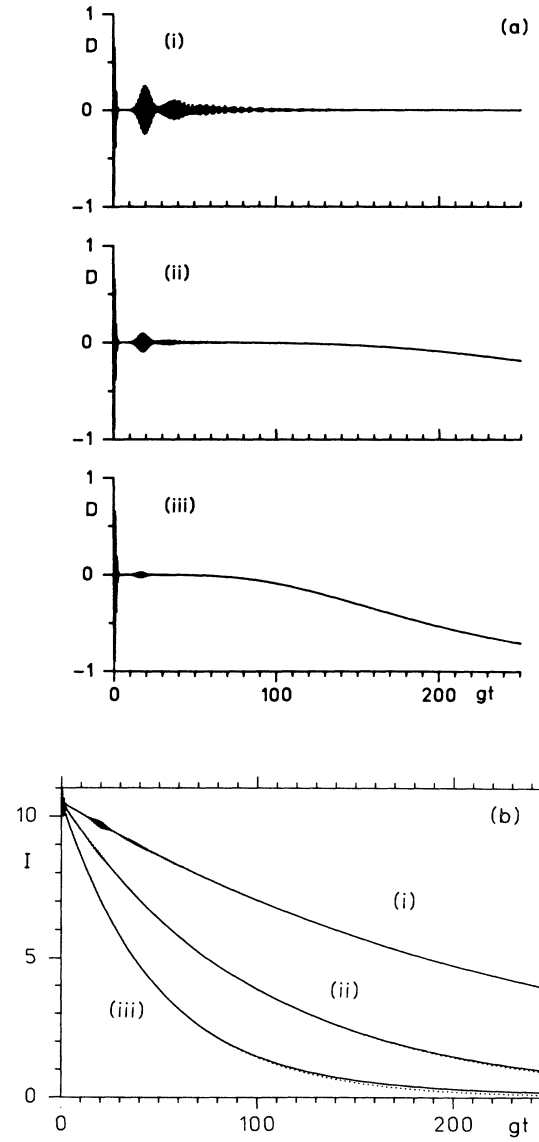

FIG. 6. (a) The inversion $D(t)$ and (b) the mean intensity $\bar{I}(t)$ as a function of gt for the damping constants (i) $\kappa/g = 0.002$, (ii) $\kappa/g = 0.005$, (iii) $\kappa/g = 0.01$ and for $\Delta = 0$, $n_{\rm th} = 0$, $\alpha_0^2 = I_0 = 10$. The dotted line in (b) is the approximation (5.2).

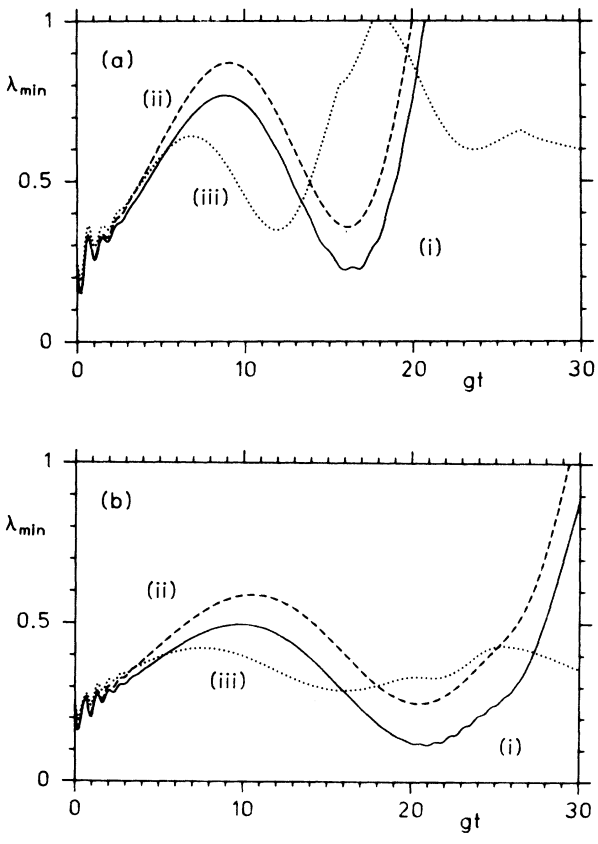

FIG. 8. (a) The minimal eigenvalue of the variance matrix of the quadrature phases as a function of gt for (i) $\kappa/g = 0.005$, $n_{\rm th} = 0.1$, (ii) $\kappa/g = 0.005$, $n_{\rm th} = 1.5$, (iii) $\kappa/g = 0.05$, $n_{\rm th} = 0.1$, and for $\alpha_0^2 = I_0 = 10$ without detuning $\Delta = 0$. (b) The minimal eigenvalue for the same parameters, but with the detuning $\Delta/g = 5$.

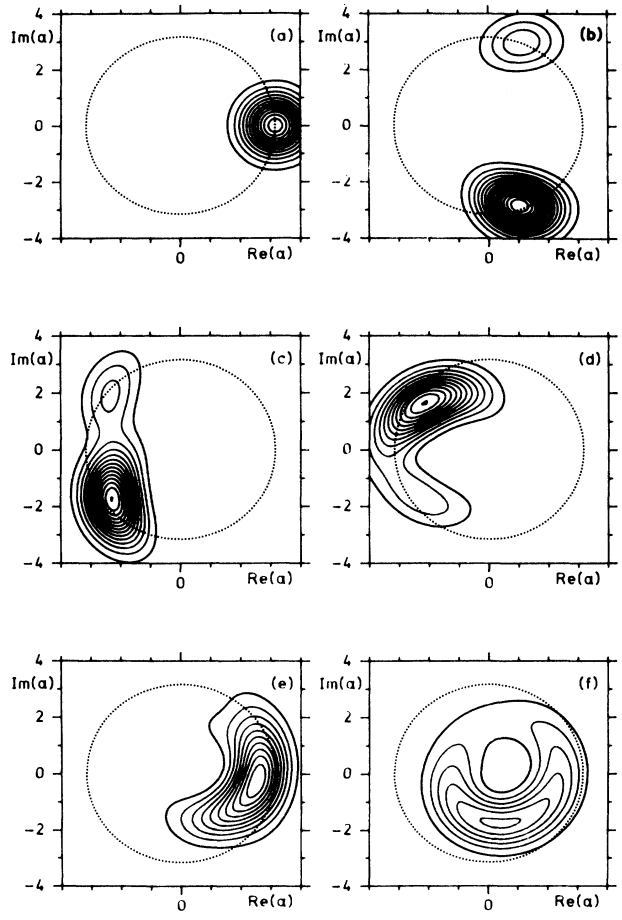

FIG. 9. Contour lines of $Q(\alpha,t) = W_1(\alpha,-1,t)$ in the complex α plane with the detuning $\Delta/g = 5$. The other parameters are the same as in Fig. 4.

the case without detuning a splitting of the initial distribution into two peaks, which counterrotate in the complex α plane, is also observed. In contrast to the case without detuning the peaks have different heights. As was already discussed in Ref. 2 for the occurrence of the revivals of the inversion, the motion is slower with detuning.

It seems to be of some interest to compare the atom-light mode interaction of the JC model with the interaction of two coupled harmonic oscillators with the same frequencies. If only the first oscillator is excited initially, all the energy goes first into the second oscillator. Then it goes back again into the first oscillator and so on. After the energy has moved back to the first oscillator the first time, the amplitude shows a phase shift of π. Such a phase shift is also observed for the JC model, see the Q function in Fig. 1 and the averaged amplitude in Fig. 7. In the JC model the atom can absorb only one photon. Thus a large initial photon energy must stay in the oscillator. The phase shift is achieved by splitting the large initial distribution. For large initial photon energies the atom needs a long time to reverse the amplitude of the oscillator.

VI. SPECIAL DISTRIBUTIONS

In this section we show how to obtain some special distributions of interest from the quasiprobability distribution. Because the density operators ρ can be expressed by the quasiprobability distributions according to[18]

$$\rho = \frac{1}{\pi}\int W(\alpha,s)e^{[\xi^*(a-\alpha)-\xi(a^\dagger-\alpha^*)-s|\xi|^2/2]}\,d^2\alpha\,d^2\xi\,, \tag{6.1}$$

any distribution, which is defined in terms of the density operator, can be expressed in terms of the quasiprobability distribution. In particular, we discuss the photon distribution, the distribution of the quadrature phases, and the phase distribution.

A. Photon distribution

The photon distribution p_n is defined by

$$p_n = \mathrm{Tr}(|n\rangle\langle n|\rho_1) = \langle n|\rho_1|n\rangle\,. \tag{6.2}$$

By inserting (6.1) into (6.2) and by using the matrix elements of the exponential operator in (6.1) listed in Appendix B one can express p_n by the parametrized distribution W_1 according to[30] ($s > -1$)

$$p_n(t) = \frac{2}{s+1}\left(\frac{s-1}{s+1}\right)^n\int_0^\infty \exp\left(-\frac{2I}{s+1}\right) \times L_n\left(\frac{4I}{1-s^2}\right) \times w_1(I,s;t)\,dI\,, \tag{6.3}$$

where L_n are the Laguerre functions and $w_1(I,s)$ is the ϕ-averaged distribution (with respect to I, w_1 is normalized to unity)

$$w_1(I,s;t) = \tfrac{1}{2}\int_0^{2\pi} W_1(I,\phi,s;t)\,d\phi\,. \tag{6.4}$$

For $s \to 1$ (6.3) specializes to the well-known result[31]

$$p_n(t) = \int_0^\infty (I^n/n!)\exp(-I)\,w_1(I,1;t)\,dI\,. \tag{6.5}$$

Insertion of the expansion (4.1) into (6.4), which in turn is inserted in (6.3), finally leads to[30]

$$p_n(t) = \pi\sum_{m=0}^{\infty}\sum_{\nu=0}^{n} c_{0,m}^{(1)}(t)\left(\frac{2\tilde{I}}{2\tilde{I}+s+1}\right)^{m+1} \times \binom{n}{\nu}\binom{m+\nu}{\nu}\left(-\frac{2}{2\tilde{I}+s+1}\right)^{\nu}\,. \tag{6.6}$$

For squeezed states W_1 and therefore also w_1 does not exist for $s = 1$. In the numerics the final result (6.6) works, however, also for $s \to 1$. As already remarked

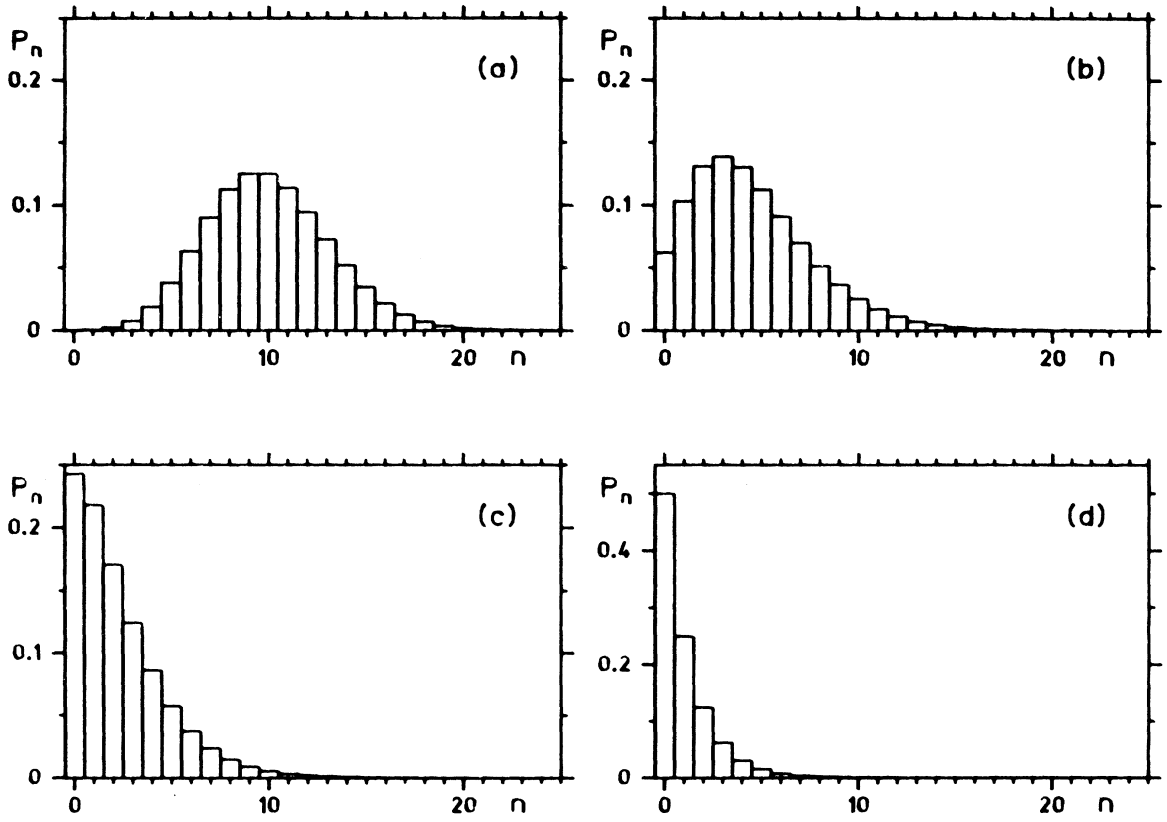

FIG. 10. The photon distribution for the times (a) $gt = 0$, (b) $gt = 10$, (c) $gt = 20$, (d) $gt = 150$. The parameters are $I_0 = 10$, $\kappa/g = 0.05$, $n_{\text{th}} = 1.0$, $\Delta = 0$.

in Sec. II, (2.8) takes also a simple form in the Fock representation. This representation leads immediately to a tridiagonally coupled system of differential equations for $p_n^{(i)} = \langle n|\rho_i|n\rangle$, which can be solved similarly as (4.2).

A typical result of the evolution of the photon distribution is shown in Fig. 10. In the course of time the initial Poisson distribution finally reaches the thermal Bose-Einstein distribution. As it should be, it is independent of the parameter s.

B. Distribution of the rotated quadrature phases

According to Refs. 32 and 33 a homodyne detector measures the following linear combinations of the creation and annihilation operators:

$$\hat{x}(\theta) = [\hat{x}(\theta)]^\dagger = (a^\dagger e^{i\theta} + a e^{-i\theta})/2 = a_r \cos\theta - a_i \sin\theta \,, \tag{6.7}$$

where the a_r and a_i are the two quadrature phases

$$a_r = (a + a^\dagger)/2 \,, \quad a_i = i(a^\dagger - a)/2 \,. \tag{6.8}$$

Though a measurement of the rotated quadrature phase inside the cavity seems to be out of the question in the experiments of Refs. 10 and 11, it is nevertheless worthwhile to discuss the distribution of this quadrature phase. Because $\hat{x}(\theta)$ is a Hermitian operator, it has a positive distribution function $w(x,\theta;t)$. This distribution can be obtained from the quasiprobability distribution. As shown recently by Vogel and one of us[34] the reverse is also true, i.e., if the probability distribution for the rotated quadrature phase is known for every θ in the interval $0 \le \theta < \pi$, then the quasiprobability can be obtained.

The explicit expression for $w(x,\theta;t)$ takes the form[34] [instead of the real and imaginary part of the integration variable we use the intensity, and the phase variable (3.4)]

$$w(x,\theta;t) = \frac{1}{4\pi} \int_0^\infty \int_0^{2\pi} \int_{-\infty}^{\infty} W_1(I, \phi+\theta, s; t) \exp[-s\eta^2/8 + i\eta(\sqrt{I}\cos\phi - x)] \, dI \, d\phi \, d\eta \,. \tag{6.9}$$

After some intermediate steps, the insertion of the expansion (4.2) leads to[30]

$$w(x,\theta;t) = \sum_{m=0}^{\infty}\sum_{n=-\infty}^{\infty} A_{n,m}\, c_{n,m}^{(1)}(t) e^{in\theta} \times H_{2m+|n|}\left(\sqrt{\frac{2}{2\tilde{I}+s}}\, x\right) \times \exp\left(-\frac{2x^2}{2\tilde{I}+s}\right) , \quad (6.10)$$

where H_n are the Hermite polynomials and where $A_{n,m}$ is an abbreviation for

$$A_{n,m} = \frac{(-1)^m 2\sqrt{\pi\tilde{I}}}{m!\sqrt{|n|!}} \left(\frac{\tilde{I}}{\tilde{I}+s/2}\right)^{m+(|n|+1)/2} . \quad (6.11)$$

Figure 11 shows a typical example of the distribution of the rotated quadrature phase for various angles θ. In Fig. 11(a) the two peaks of the Q function are very well separated. For zero θ we see pronounced oscillations whereas for $\theta = \pi/2$ we see a two-peak structure. In Fig. 11(b) the two peaks of the Q function have collided. Here we have one small peak for zero θ and a broader one for $\theta = \pi/2$.

C. Phase distribution

A prescription for a Hermitian phase operator, which has the required properties of a phase operator (see for instance Ref. 35), was recently given by Pegg and Barnett.[36,37] In the Fock representation for the states $|\theta_m\rangle$ their discrete distribution for the phase [see (6.9) in Ref. 37] leads in the limit of a very large number of states to the continuous phase distribution

$$P(\phi,t) = \frac{1}{2\pi}\sum_{m,n=0}^{\infty} \langle m|\rho_1(t)|n\rangle \exp[i(n-m)\phi] . \quad (6.12)$$

Here the phase distribution is normalized to one for ϕ in the interval $(0, 2\pi)$. For the pure state $\rho_1 = |\psi_{sq}\rangle\langle\psi_{sq}|$, (6.12) reduces to the phase distribution (4) and (6) of Ref. 38 or (3.4) and (3.5) of Ref. 39. By inserting the density operator (6.1), by using the matrix elements (B1) and Ref. 26 we can express the phase distribution by the quasiprobability distribution according to ($s > -1$)

$$P(\phi,t) = \tfrac{1}{2}\int_0^{\infty}\int_0^{2\pi} K(I,\phi-\phi',s) W_1(I,\phi',s;t)\, dI\, d\phi . \quad (6.13)$$

Here the kernel K has the form

$$K(I,\phi-\phi',s) = \frac{1}{2\pi}\sum_{n,m=0}^{\infty} \exp[i(n-m)(\phi-\phi')] B_{m,n} , \quad (6.14)$$

where the coefficients $B_{m,n}$ for ($m \geq n$) are given by

$$B_{m,n} = \sqrt{\frac{n!}{m!}}\, I^{(m-n)/2}\left(\frac{s-1}{2}\right)^n \left(\frac{s+1}{2}\right)^{-m-1} \times L_n^{(m-n)}\left(\frac{4I}{1-s^2}\right)\exp\left(-\frac{2I}{1+s}\right) , \quad (6.15)$$

see also (6.51) of Ref. 40 (here one has to replace s by $-s$). The coefficients $B_{m,n}$ for $m \leq n$ follow from

$$B_{m,n} = B_{n,m} . \quad (6.16)$$

In the limit $s \to 1$ the B coefficients specialize to

$$B_{m,n} = I^{(m+n)/2} e^{-I}/\sqrt{m!\,n!} . \quad (6.17)$$

Then the corresponding kernel is the phase distribution (6.12) for the coherent state $|\sqrt{I}\exp(i\phi')\rangle$.

By inserting in (6.13) the sum (4.1), the phase distribution can thus be obtained. The lengthy expression contains four sums[41] and will not be given here. In Fig. 12 some typical phase distributions are shown. As time increases the one-peak structure splits into a two-peak structure. For large times it reaches a constant distribution.

Sometimes it is said that the phase distribution $P(\phi)$ cannot be measured and is therefore only of theoretical interest. As was shown recently by Vogel and one of us[34] the quasiprobability can be expressed in terms of the rotated quadrature phase, which can be measured. Because of (6.13), the phase distribution can thus also be measured in principle.

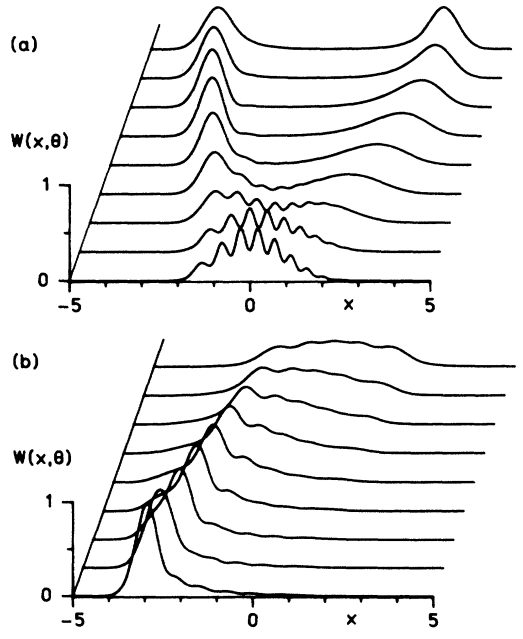

FIG. 11. The distribution $w(x,\theta;t)$ of the rotated quadrature for the angles $\theta = 0$ (lowest curve), $1\pi/16$, $2\pi/16$, ..., $8\pi/16$ (upper-most curve) and for (a) $gt = 10$ and (b) $gt = 20$. The other parameters are the same as in Fig. 4.

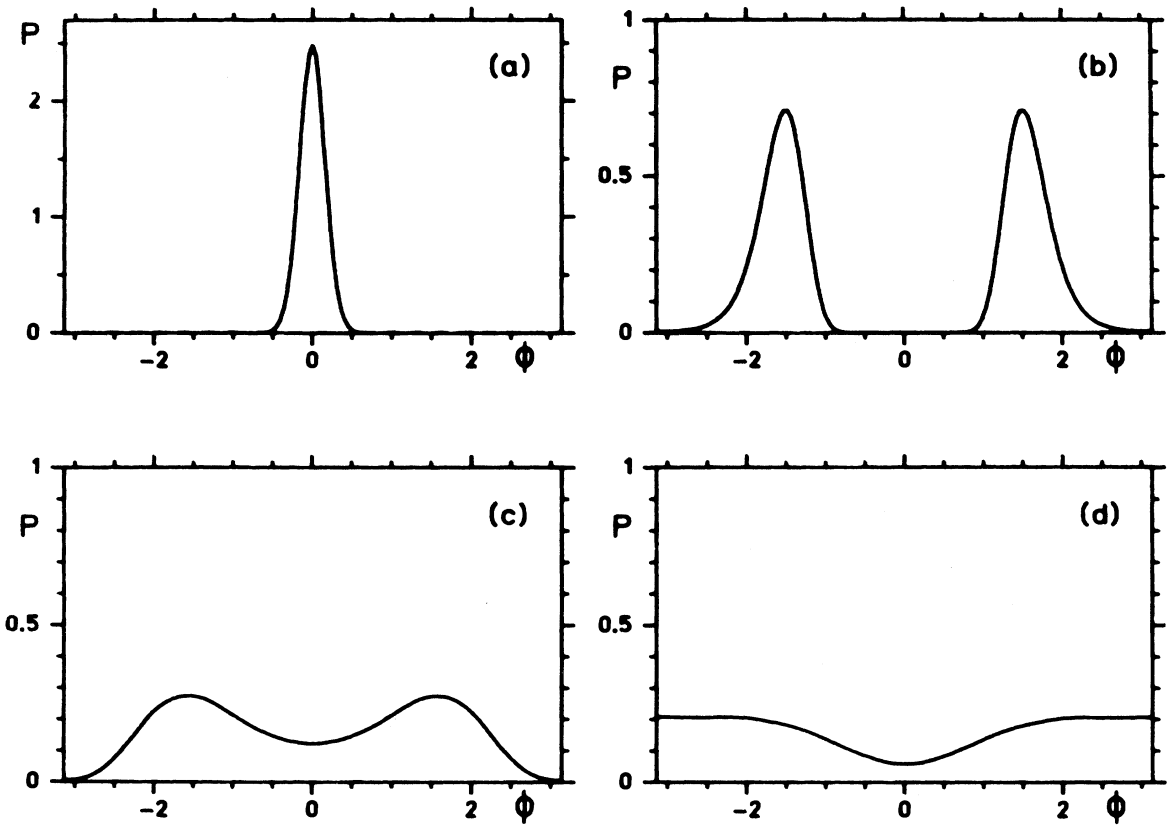

FIG. 12. The phase distribution $P(\phi, t)$ for (a) $gt = 0$, (b) $gt = 10$, (c) $gt = 30$, (d) $gt = 50$. The other parameters are the same as in Fig. 4.

VII. SUMMARY

The quasiprobability distributions for the Jaynes-Cummings model with cavity damping have been obtained. The first main step of our procedure has been the introduction of six suitable combinations of the four density operators, i.e., of the four atomic matrix elements. By introducing quasiprobability distributions for each of the six combinations the equation of motion has been transformed into a system of partial-differential equations. By expanding the distributions into two complete sets, a system of ordinary differential equations has been obtained for the expansion coefficients. This system is tridiagonally coupled in only one index, which simplifies the numerical procedure considerably. For the final integration a Runge-Kutta method was used, which was specially adapted to the tridiagonal form. In this way various quasiprobability functions (Q and Wigner function), mean intensity and inversion, as well as the photon distribution, the distribution of the rotated quadrature phase, and the phase distribution have been obtained.

The main result of our investigation is the splitting of the quasiprobabilities. If we start with a coherent state, i.e., with a shifted Gaussian quasiprobability distribution, this distribution splits into two peaks counterrotating in the complex plane. Rabi oscillations of the inversion are observed initially and when the two peaks collide, during the splitting the Rabi oscillations disappear.

The present investigation can be extended into several directions. We may use, for instance, different initial conditions. One may start with a thermal light field or with a shifted squeezed field instead of the coherent field always assumed in this paper. For the last initial condition ringing revivals of the Rabi oscillations have been found by Satyanarayana *et al.*[42] Preliminary investigations show that in this case also a splitting occurs, each of the two peaks having, however, a more complicated structure. We may also treat the case of the micromaser, in which a new excited atom is injected into the cavity and the previous one is removed. An approximate theory has been developed by Krause *et al.*,[43] where cavity damping was neglected during the time, in which the atom is in the cavity. With the present method this problem can be treated without switching off the cavity damping. Here we have to start the system (4.2) again every time a new atom is injected in the cavity. The previous density operator of the light field operator is then used as the light operator for the new initial condition. In this way the buildup of the light inside the cavity and its dependence on the damping constant and the thermal photon number

can be investigated.

So far we have assumed that initially the atom is in its upper state. If we take as initial conditions those which correspond to only one of the split peaks, nondiagonal elements of the atom density operators have to be taken into account. In this case only one peak is moving around and revivals of the Rabi oscillations do not occur.

A more complicated model than the JC model may also be treated by the method presented in this paper. We may, for instance, consider more eigenstates of the atom or we may even treat the case of two or more atoms. A multiphoton JC model may also be treated. Hilsenbeck and one of us[44] have applied the method to a two-photon JC model with cavity damping. In this system a splitting of the quasiprobability is also observed.

ACKNOWLEDGMENTS

We would like to thank G. S. Agarwal, P. L. Knight, S. J. D. Phoenix, and W. Schleich for useful discussions and C. Miller for reading the manuscript. The financial support of the Deutsche Forschungsgemeinschaft (DFG) is also greatly acknowledged.

APPENDIX A: Q FUNCTION WITHOUT DAMPING

Starting with an initially coherent state $|\alpha_0\rangle$ ($\alpha_0 = \sqrt{I_0}$) in the upper state of the atom, the solution of the Schrödinger equation with the Hamilton operator (2.5) takes the form[1,23]

$$|\psi(t)\rangle = \exp(-I_0/2)\sum_{n=0}^{\infty}\frac{{\alpha_0}^n}{\sqrt{n!}}\,[A_n(t)|n\rangle|\uparrow\rangle + B_n(t)|n+1\rangle|\downarrow\rangle]\,, \tag{A1}$$

where the functions $A_n(t)$ and $B_n(t)$ read

$$A_n(t) = \cos(\lambda_n t) - i\frac{\Delta}{2\lambda_n}\sin(\lambda_n t)\,, \tag{A2}$$

$$B_n(t) = -i\frac{\sqrt{n+1}\,g}{\lambda_n}\sin(\lambda_n t)\,,$$

with λ_n given by

$$\lambda_n = \sqrt{\Delta^2/4 + (n+1)g^2}\,. \tag{A3}$$

The Q function of the light field is defined by

$$Q(\alpha,t) = W_1(\alpha,-1;t) = \mathrm{Tr}_A[\langle\alpha|\rho(t)|\alpha\rangle]/\pi\,, \tag{A4}$$

where the density operator is expressed by the wave function according to $\rho(t) = |\psi(t)\rangle\langle\psi(t)|$. Insertion of (A1) leads to

$$Q(\alpha,t) = (|V_A|^2 + |V_B|^2)/\pi \tag{A5}$$

with V_A and V_B given by

$$V_A = \exp\left(-\frac{I_0}{2} - \frac{|\alpha|^2}{2}\right)\sum_{n=0}^{\infty}\frac{(\sqrt{I_0}\,\alpha^*)^n}{n!}A_n(t)\,,$$

$$V_B = \exp\left(-\frac{I_0}{2} - \frac{|\alpha|^2}{2}\right)\sum_{n=0}^{\infty}\frac{(\sqrt{I_0}\,\alpha^*)^n}{n!}\frac{\alpha^*}{\sqrt{n+1}}B_n(t)\,. \tag{A6}$$

By approximating the sums by integrals similarly as done for the inversion in Ref. 2, analytical expressions for the Q function can also be derived. Without detuning one thus obtains in a first approximation[19]

$$Q(\alpha,t) = Q_+(\alpha,t) + Q_-(\alpha,t)\,, \tag{A7}$$

with

$$Q_\pm = N\exp(-ax^2 \pm 2bxy_\pm - c{y_\pm}^2)\,;$$

$$x = |\alpha| - \alpha_0\,,\quad y_\pm = \alpha_0(\phi \pm \tau)\,. \tag{A8}$$

The quantities N, a, b, c are expressed in terms of the normalized time

$$\tau = gt/(2\alpha_0) \tag{A9}$$

according to

$$c = \frac{4}{4+\tau^2}\,,\quad a = 2-c\,,\quad b = \frac{\tau}{2}c\,,\quad N = \frac{1}{\pi\sqrt{4+\tau^2}}\,. \tag{A10}$$

The contour lines of (A8) are ellipses. They fit quite well with those of Fig. 1(a). The angle γ between the major axis of the ellipses and the tangent to the circle $|\alpha| = \alpha_0$ is given by $\tan(2\gamma) = 2/\tau$. The width of each of the $Q_\pm$ functions can easily be obtained from the eigenvalues $\lambda_{\frac{1}{2}}$ of the quadratic form in (A8). They are given by

$$\lambda_{\frac{1}{2}} = 1 \pm \tau/\sqrt{4+\tau^2}\,. \tag{A11}$$

If τ is not too large, each of the $Q_\pm$ functions in (A8) describes the Q function of a squeezed state. For a proper rotated coordinate system the squeezing parameter C ($|C| \le 1/2$), as defined in Ref. 45, is given by

$$C = \tau/(2\sqrt{4+\tau^2})\,. \tag{A12}$$

Thus for $\tau > 0$ one obtains an appreciable amount of squeezing for each of the $Q_\pm$ functions.

The approximate expressions (A7) and (A8) do not show the fluctuations of the peaks as seen in Fig. 2. A

more accurate approximation analysis,[46] however, also reveals these fluctuations. The analysis explains that the fluctuations of the peaks and the Rabi oscillations of the inversion disappear if the two peaks do not overlap. In Ref. 46 the long-time behavior is also investigated.

APPENDIX B: MATRIX ELEMENTS OF THE EXPONENTIAL OPERATOR

The matrix elements of the exponential operator occurring in (6.1) with respect to the Fock states are given by[40]

$$\langle m|\exp(\xi^* a - \xi a^\dagger)|n\rangle = \exp(-|\xi|^2/2) \times \begin{cases} \sqrt{n!/m!}\,(-\xi)^{m-n} L_n^{(m-n)}(|\xi|^2) & \text{for } m \geq n \\ \sqrt{m!/n!}\,(\xi^*)^{n-m} L_m^{(n-m)}(|\xi|^2) & \text{for } n \geq m\,. \end{cases} \tag{B1}$$

If we use generalized Laguerre polynomials with a negative upper index as defined on p. 240 of Ref. 25, we do not need to distinguish between the case $m \geq n$ and $m \leq n$.

[1] E. T. Jaynes and F. W. Cummings, Proc. Inst. Electr. Eng. **51**, 89 (1963).
[2] J. H. Eberly, N. B. Narozhny, and J. J. Sanchez-Mondragon, Phys. Rev. Lett. **44**, 1323 (1980).
[3] S. M. Barnett, P. Filipowicz, J. Javanainen, P. L. Knight, and P. Meystre, in *Nonlinear Phenomena and Chaos*, edited by S. Sarkar and E. R. Pike (Hilger, London, 1986), p. 485.
[4] P. Filipowicz, J. Phys. A **19**, 3785 (1986).
[5] G. S. Agarwal, J. Opt. Soc. Am. B **2**, 480 (1985).
[6] A. Bandilla and H. H. Ritze, IEEE J. Quantum Electron. **24**, 1338 (1988).
[7] P. Meystre and M. S. Zubairy, Phys. Lett. **89A**, 390 (1982).
[8] P. K. Aravind and G. Hu, Physica C **150**, 427 (1988).
[9] M. Hillery, Phys. Rev. A **39**, 1556 (1989).
[10] G. Rempe, H. Walther, and N. Klein, Phys. Rev. Lett. **58**, 353 (1987).
[11] F. Diedrich, J. Krause, G. Rempe, M. O. Scully, and H. Walther, IEEE J. Quantum Electron. **24**, 1314 (1988).
[12] P. Knight, Phys. Scr. T **12**, 51 (1986).
[13] L. Schoendorff and H. Risken, Phys. Rev. A **41**, 5147 (1990).
[14] S. M. Barnett and P. L. Knight, Phys. Rev. A **33**, 2444 (1986).
[15] R. R. Puri and G. S. Agarwal, Phys. Rev. A **35**, 3433 (1987).
[16] J. R. Kuklinski and J. L. Madajczk, Phys. Rev. A **37**, 3175 (1988).
[17] N. Nayak, R. K. Bullough, B. V. Thompson and G. S. Agarwal, IEEE J. Quantum. Electron. **24**, 1331 (1988).
[18] K. E. Cahill and R. J. Glauber, Phys. Rev. **177**, 1882 (1969).
[19] H. Risken (unpublished).
[20] S. J. D. Phoenix and P. L. Knight, J. Opt. Soc. Am. B **7**, 116 (1990).
[21] J. Eiselt and H. Risken, Opt. Commun. **72**, 351 (1989).
[22] H. Risken and J. Eiselt (unpublished).
[23] P. Meystre and M. Sargent, *Elements of Quantum Optics* (Springer, Berlin, 1990).
[24] K. Vogel and H. Risken, Phys. Rev. A **39**, 4675 (1989).
[25] W. Magnus, F. Oberhettinger, and R. P. Soni, *Formulas and Theorems for the Special Functions of Mathematical Physics* (Springer, Berlin, 1966).
[26] A. P. Prudnikov, Yu. A. Brychkov, and O. I. Marichev, *Integrals and Series, Vol.2: Special Functions* (Gordon and Breach, New York 1986), p. 474, integral 2.19.12.6.
[27] W. H. Press, B. P. Flannery, S. A. Teukolsky, and W. T. Vettering, *Numerical Recipes* (Cambridge University Press, Cambridge, 1986).
[28] H. Risken, in *The Fokker-Planck Equation*, 2nd ed., Vol. 18 of *Springer Series in Synergetics*, edited by H. Haken (Springer, Berlin, 1989).
[29] W. Schleich and M. Pernigo (unpublished).
[30] K. Vogel, Ph.D. thesis, Ulm, 1989.
[31] L. Mandel and E. Wolf, Phys. Rev. **124**, 1696 (1961).
[32] H. P. Yuen, J. H. Shapiro, IEEE Trans. Inf. Theory **26**, 78 (1980).
[33] B. Yurke and D. Stoler, Phys. Rev. A **36**, 1955 (1987).
[34] K. Vogel and H. Risken, Phys. Rev. A **40**, 2847 (1989).
[35] P. Caruthers and M. M. Nieto, Rev. Mod. Phys. **40**, 411 (1968).
[36] D. T. Pegg and S. M. Barnett, Europhys. Lett. **6**, 483 (1988).
[37] D. T. Pegg and S. M. Barnett, Phys. Rev. A **39**, 1665 (1989).
[38] W. Schleich, R. J. Horowicz, and S. Varro, Phys. Rev. A **40**, 7405 (1989).
[39] W. Schleich, R. J. Horowicz, and S. Varro, in *Quantum Optics V*, edited by J. D. Harvey and D. F. Walls (Springer, Berlin, 1989), p. 133.
[40] K. E. Cahill and R. J. Glauber, Phys. Rev. **177**, 1857 (1969).
[41] J. Eiselt, Ph.D. thesis, Ulm, 1990.
[42] M. V. Satyanarayana, P. Rice, R. Vyas, and H. J. Carmichael, J. Opt. Soc. Am. B **6**, 228 (1989).
[43] J. Krause, M. O. Scully, T. Walther, and W. Walther, Phys. Rev. A **39**, 1915 (1989).
[44] J. Hilsenbeck and H. Risken (unpublished).
[45] H. P. Yuen, Phys. Rev. A **13**, 2226 (1976).
[46] C. Miller and H. Risken (unpublished).